PHYSICAL REVIEW A VOLUME 2, NUMBER 5 NOVEMBER 1970

Measurements of Excited-State Population Ratios of Atomic Hydrogen Produced by Charge-Exchange Neutralization of Energetic Proton Beams*

Robert H. McFarland† and Archer H. Futch, Jr.
Lawrence Radiation Laboratory, University of California, Livermore, California 94550
(Received 10 April 1970)

Excited-state population ratios for atomic hydrogen have been measured for energetic hydrogen ions neutralized by charge exchange with a number of different metallic vapors and permanent gases. Electric field ionization techniques were used to determine excitation ratios. Detection of the energetic ions and neutrals was accomplished using partially depleted surface-barrier detectors. Counting, using phase-detection techniques in which an add-subtract scaler was phased to the signal, provided an improved signal-to-noise ratio. Two methods were used to provide desired targets. Metallic vapor and permanent-gas thin targets of the order of 10^{-5} mTorr cm were produced as chopped neutral beams, using conventional crossed-beam techniques. Gas cells were used to extend these measurements with permanent gases to targets up to seven orders of magnitude thicker. In the latter case, the ion beam was interrupted electrically. Targets investigated were magnesium, potassium, barium, hydrogen, nitrogen, thallium, Freon, water vapor, ammonia, and perfluorodimethylcyclohexane (C_8F_{16}).

INTRODUCTION

The ionization of neutral hydrogen atoms by Lorentz force provides a mechanism for trapping energetic particles inside plasma-containment devices. This technique, as well as procedures for measuring excited-state populations by use of electric field ionization, has been previously described by many authors.[1-9] The threshold electric field $\vec{E}$ or equivalent Lorentz field $\vec{v}\times\vec{B}$ required to ionize the nth level of the hydrogen atom is equal to b/n^4, where the parameter b is determined from experimental measurements of the threshold electric field. The fraction $R(n)$ of excited atoms in a higher quantum level n produced by charge exchange on an appropriate target is assumed to be expressed by the formula

$$R(n) = \alpha/n^3 \ , \tag{1}$$

where α is an energy-dependent parameter which depends on the nature of the charge-exchange target. From the n dependence of both the threshold electric field and the excited-state population, it has been shown that the ratio of ions produced by the electric field to total neutrals is proportional to the square root of the ionizing field.[9] That is, we obtain

$$\int_n^\infty R(n')dn' = (\alpha/2\sqrt{b})\sqrt{E} = 6.4\times10^{-4}\alpha\sqrt{E} \ . \tag{2}$$

For thin targets, $R(n)$ is given by the ratio

$$R(n) = \alpha_0/n^3 = \sigma_n^c/\sum_{n'}\sigma_{n'}^c \ , \tag{3}$$

where σ_n^c is the probability of a charge-exchange interaction leaving the neutral atom in the nth excited state.

At this time, authors have chosen to express their results in terms of the thin-target excitation coefficient α_0, the excitation coefficient for thick targets α, and $R(11)$ or $R(14)$, which are α_0 (or α) divided by $(11)^3$ and $(14)^3$, respectively. These latter results have had significance in connection with their use in the neutral-injection technique as have the thick-target α values.

This paper describes recent excitation measurements on metallic vapors involving targets of the order of 10^{-5} mTorr cm thick and permanent gas targets ranging from 10^{-5} to 10^3 mTorr cm thick.

APPARATUS AND METHOD

Figure 1 indicates schematically the crossed-beam method used for thin-target measurements. Energy-analyzed ions enter the high-vacuum chamber through three sets of deflector plates biased to pass the ions but to block neutrals formed in the higher-pressure beam-pipe region. After passing through a 250-mil aperture 1, the ion beam passes through a 1-cm-thick chopped neutral beam at position 2 and is then deflected out of the beam path by an electric field of less than 250 V/cm. Apertures 3–5 (250-mil diam) are used for measuring and defining the beam. The aperture in electrode 6 is 5 mils in diam, which limits the magnitude of the neutral beam passing through the subsequent 8-mil apertures 7 and 8. These apertures, 16 mil apart, constitute the electric field ionizer. The ion and neutrals leaving the ionizer are separated by an electric field, after which one may either count the ions and neutrals together or only the ions representing the excited atoms ionized by the electric field.

The full width at half-maximum (FWHM) resolution of the surface-barrier detector has been ob-

① Defining aperture.
② Neutral crossed beam with collector plates above and below.
③ Electrode for observing focusing and scattering
④ Grounded aperture, 250 mil.
⑤ Biased aperture for measuring ions.
⑥ Faraday cup with 5-mil aperture.
⑦ and ⑧ Lorentz ionizer, 8-mil apertures, 16-mil separation.

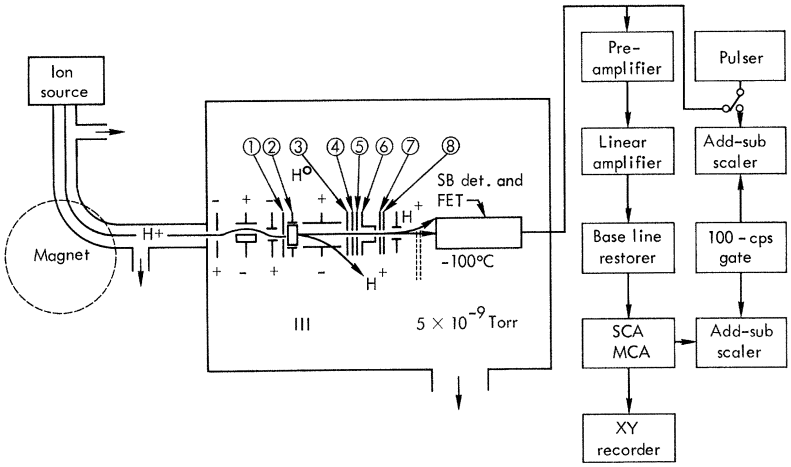

FIG. 1. Schematic diagram of the ion-beam production, crossed-beam neutralizer, Lorentz ionizer, and particle detector.

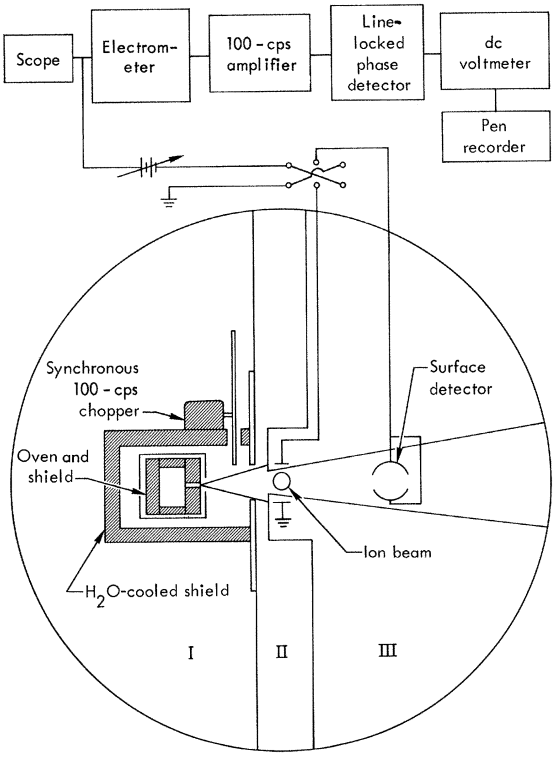

FIG. 2. Schematic diagram of neutral-beam production. Background and operating pressures were 5×10^{-9} and 1×10^{-8} Torr, respectively.

served as low as 2.8 keV at 10-keV particle energy. The signal was amplified and then analyzed by a 100-channel analyzer. The multichannel display is recorded while the single-channel response is differentially analyzed and recorded with an add-subtract scaler phased to the 100-cps chopped neutral beam. The second add-subtract scaler, fed by a 5-kc/sec pulser and using the same 100-cps square wave gate signal, is used for maintaining the gating symmetry at better than one part in a thousand.

The differentially pumped vacuum system for producing the 100-cps neutral beam is shown in Fig. 2.

Figure 3 shows in more detail the ionizer and the beam resulting from the passage of a neutral beam through the electric field.

A second mode of operation for thick-target measurements involved installing a 92-cm gas cell with 100-mil apertures just in front of aperture 1, Fig. 1. Pressures within the cell were measured from about 10^{-3} to 10^{-5} Torr by use of a Baratron. Ionization gauges were used for extending the pressure measurements to still lower values. In this mode of operation, the ion beam was electrically interrupted at 100-cps prior to the gas cell in order that background detector noises be eliminated through phase detection. In all measurements statistical probable errors were kept to less than 10%.

Since the maximum effective distance that the neutrals travel after neutralization is of the order of 50 cm, one must be somewhat concerned about radiative losses subsequent to neutralization. In

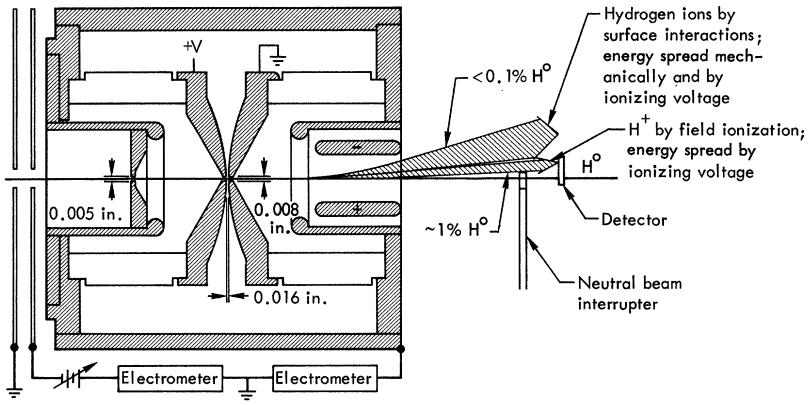

FIG. 3. Lorentz ionizer.

the earth's magnetic field, the Lorentz field $\vec{v}\times\vec{B}$ is such that Stark lifetimes must be used. Radiative decay corrections using Stark lifetimes[10] (statistically averaged over all substates) were less than 10% for the least energetic particles (4 keV). This correction decreases with increasing energy and has been neglected in the present measurements. Losses due to base pressures of the order of 10^{-8} Torr in the post-collision regions were also neglected.

Ion-accelerating voltages and magnetic fields were monitored using differential voltmeters and held to variations of less than one part per thousand. Consistency measurements were made after each experimental change to ensure that the excitation ratio was proportional to $E^{1/2}$.

Figure 4 presents thin-target measurements made on magnesium.

RESULTS AND DISCUSSION

Thin Targets Using Crossed-Beam Techniques

Thin-target measurements are especially meaningful in comparing theory with experiment to confirm understanding of the process involved. Figures 5–8 display $R(11)$ values for energies ranging from 5 to 35 keV for barium, potassium, magnesium, and thallium. Thin-target α values may be obtained by multiplying $R(11)$ by 1331. The most extensive experimental measurements have been made using magnesium, with good agreement between the results of different experimentalists.

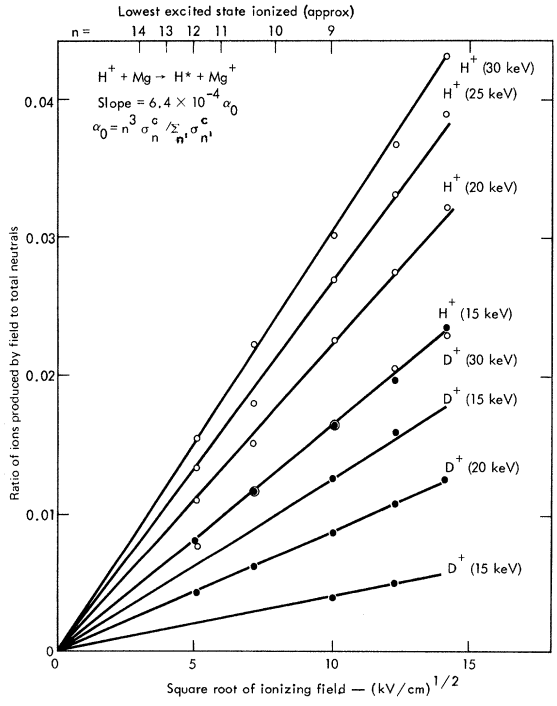

FIG. 4. Typical R values plotted as a function of $E^{1/2}$. After necessary consistency checks, linearity was assumed and subsequent measurements were made at $E = 10^5$ V/cm.

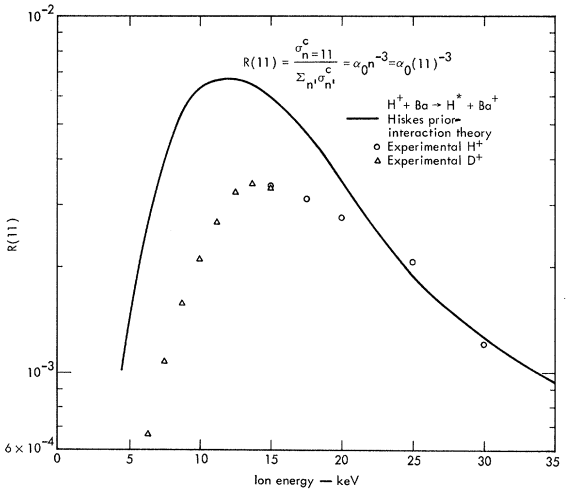

FIG. 5. Thin-target excited-state coefficient measurements for barium as a function of proton equivalent energy.

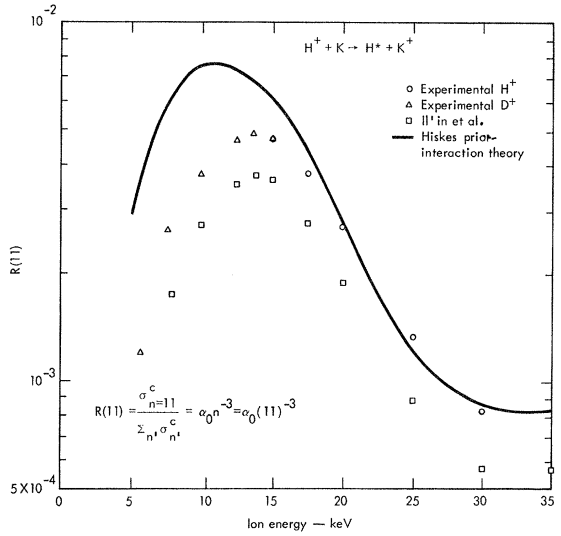

FIG. 6. Thin-target excited-state coefficient measurements for potassium as a function of proton equivalent energy.

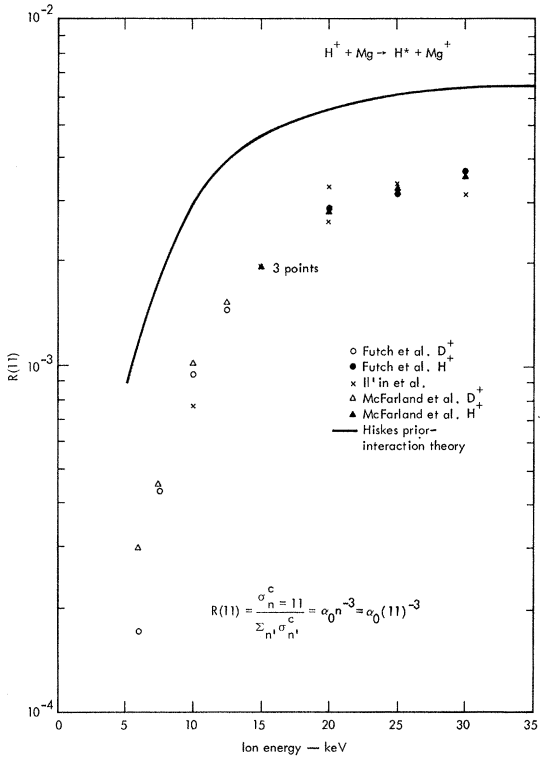

FIG. 7. Thin-target excited-state coefficient measurements for magnesium as a function of proton equivalent energy.

Although theoretical predictions of $R(n)$ based on prior-interaction theory are somewhat greater than measurements, it should be remembered that this theory, using wave functions describing the particles prior to the collision, is only an approximation to the actual collision. While it is possible to average prior- and post-interaction calculations and obtain somewhat better agreement between experiment and theory, it is generally agreed that prior theory agrees remarkably well with experimentation. The accuracy of measurement of $R(11)$ and/or α_0 is enhanced by the fact that they are ratios of two measurements made in the same manner, so that any inaccuracies in the measurements tend to cancel. This is also true to an extent with the calculations, resulting in reduced need for precise wave functions.

Barium, because of its chemical activity and physical properties, has not been measured despite the previous efforts by Il'in and co-workers; consequently, previous experimental values are not available for comparison. Its agreement with prior interaction theory is reasonable. There is no previous work on thallium available for comparison. Its most interesting feature lies in its possible use as a neutralizer at low energies.

Thin- and Thick-Target Measurements Using Gas-Cell Techniques

Permanent gases lend themselves to gas-cell usage with the possibility of extending the target thickness to values normally useful for neutral-particle injection. While thin targets represent conditions for single collisions and extend from about 10^{-5} to 1 mTorr cm, thick targets are more difficult to define. In general, however, thick targets provide for multiple collisions with equilibrium being reached between the competitive processes involving ionization, excitation, and loss of excitation.

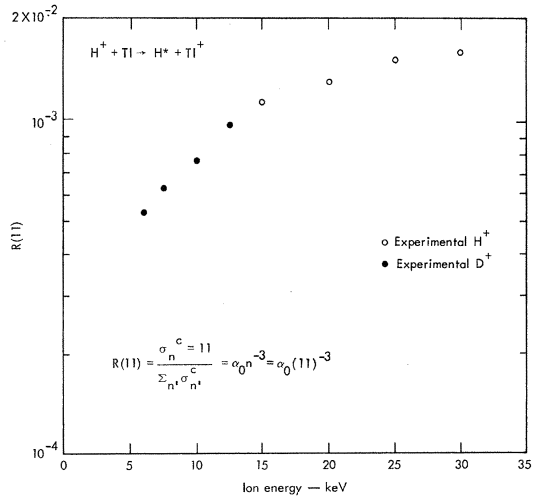

FIG. 8. Thin-target excited-state coefficient measurements for thallium as a function of proton equivalent energy.

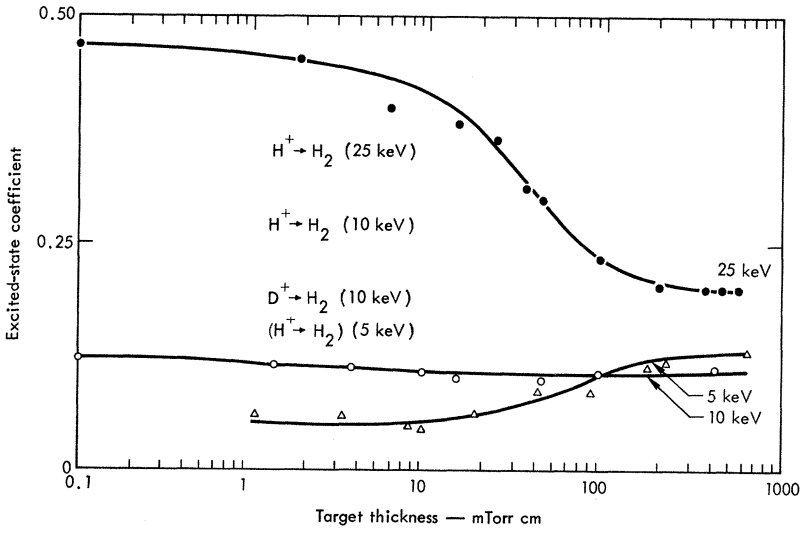

FIG. 9. Variable-thickness-target excited-state coefficient measurements α for three proton equivalent energies with a H_2 target.

TABLE I. Compilation of measurements of thin- and thick-target excitation coefficients. Numbers in parentheses are target thicknesses (maximum neutral production) in mTorr cm.[a]

Energy (keV)	4		5		6		7.5		10		12.5		15		20		25		30	
Molecule	α_0	α	α_0	α	α_0	α	α_0	α	α_0	α	α_0	α	α_0	α	α_0	α	α_0	α	α_0	α
Ba	···	···	···	···	0.89	···	1.4	···	2.7	···	4.3	···	4.4	···	3.7	···	2.7	···	1.6	···
K	···	···	···	···	1.6	···	3.5	···	5.1	···	6.3	···	6.3	···	3.6	···	1.8	···	1.1	···
Mg	···	···	···	···	0.4	···	0.6	···	1.3	···	2.0	···	2.6	···	3.7	···	4.3	···	4.7	···
Tl	···	···	···	···	0.72	···	0.84	···	1	···	1.3	···	1.5	···	1.7	···	2	···	2.1	···
				(200)																
H_2	···	···	0.06	0.12	···	···	···	···	0.15	0.11	···	···	0.28	···	0.45	0.27	0.53	0.2	0.64	···
				(270)						(50)										
N_2	···	···	0.1	0.19	···	···	···	···	0.16	0.3	···	···	0.23	···	0.46	···	0.51	···	0.60	···
		(150)		(140)		···		···		···		(80)		(70)		(50)		(40)		
C_8F_{16}	>1.0	0.38	0.8	0.35	0.41	···	0.38	···	0.36	···	0.38	0.25	0.41	0.25	0.55	0.30	>0.6	0.33		
Freon 114	···	···	···	···	0.27	···	0.31	···	0.47	···	0.57	···	0.68	···	0.80	···	0.93	···	1.0	···
				(60)																
H_2O			0.08	0.13																
				(380)																
NH_3			0.1	0.15																

[a] These pressures were calibrated against a Baratron. There is some reason to believe that for C_8F_{16} the absolute magnitude may be in error; however, the relative values should be significant.

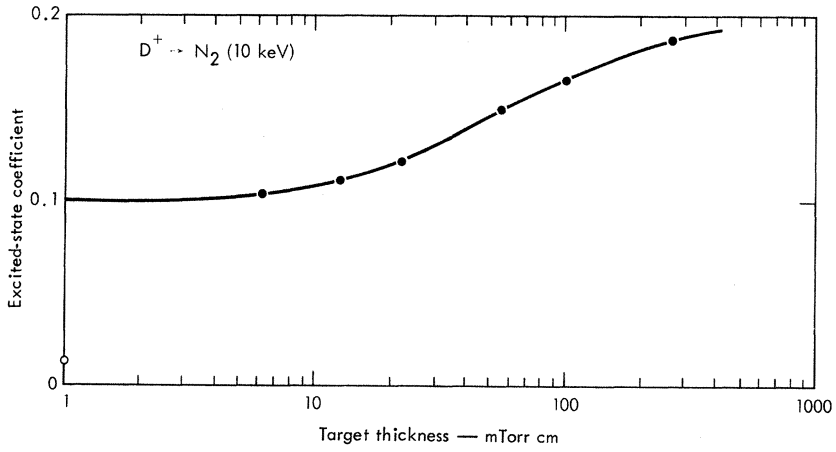

FIG. 10. Variable-thickness-target excited-state coefficient measurements α for a proton equivalent energy of 5 keV and with N_2 as the target.

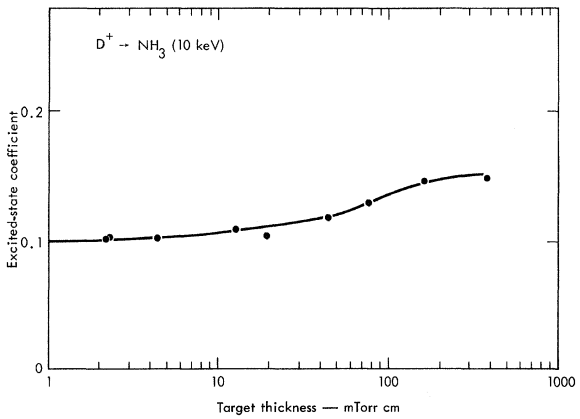

FIG. 11. Variable-thickness-target excited-state coefficient measurements α for a proton equivalent energy of 5 keV and with NH_3 as the target.

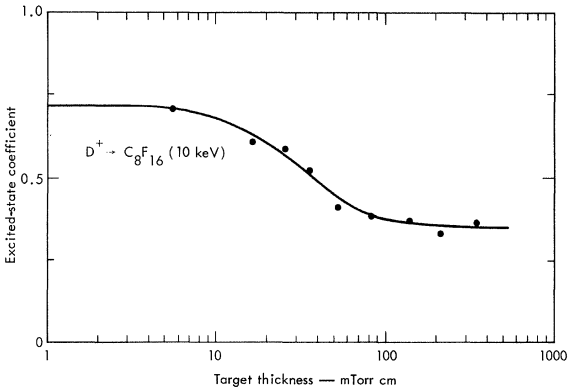

FIG. 13. Variable-thickness-target excited-state coefficient measurements α for a proton equivalent energy of 5 keV and with C_8F_{15} as the target. Optimal thickness may be determined from the production of the field ionized and/or total neutrals.

Further, one normally chooses an optimum-thickness target for neutralization of a beam because a still thicker target causes undesirable scattering from the beam. Figure 9 summarizes measurements of α for H^+ on H_2 made at three different energies. The 25-keV results are typical of previous measurements showing a decrease in the excited-state coefficient α as the target thickness is increased. The net effect of multiple collisions on a highly excited n level depends on a competition between processes which tend to populate the level (charge exchange, excitation, and deexcitation) and those which tend to depopulate the level (ionization, excitation, and deexcitation). At 25 keV competition between these processes in hydrogen gas leads to depopulation as the target thickness increases. As the energy is reduced, processes which populate an excited level become stronger than processes which depopulate. The net result of multiple collisions at 5-keV energies is to enhance the population of highly excited levels as the target thickness increases.

Additional measurements with other gases show that the enhancement of the highly excited levels by multiple collisions is a general characteristic of many gases at low energies. The variation of the excited-state coefficient α as a function of target thickness is shown in Figs. 10–12 for the gases N_2, NH_3, and H_2O, respectively. All three gases show an increase in α as the target thickness is increased. Perfluorodimethylcyclohexane (C_8F_{16}) as shown in Fig. 13 does not exhibit this characteristic at a comparable energy. In earlier results,

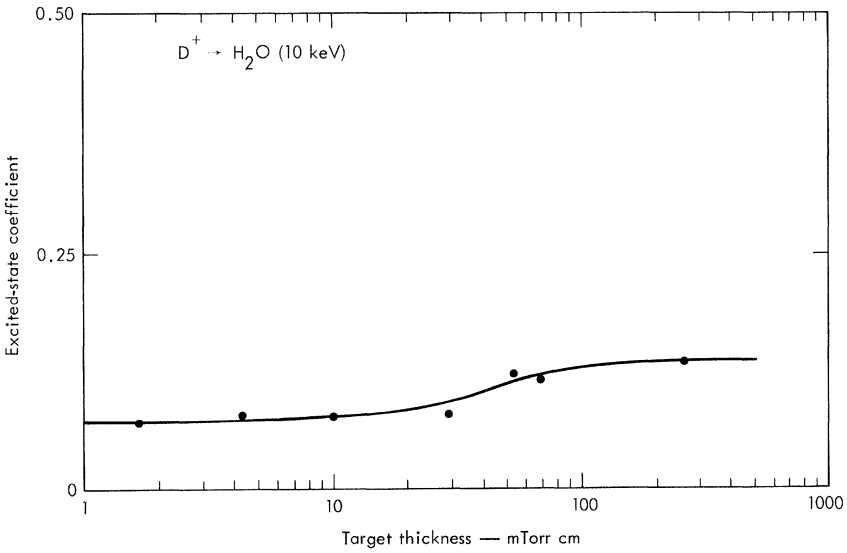

FIG. 12. Variable-thickness-target excited-state coefficient measurements α for a proton equivalent energy of 5 keV and with H_2O as the target.

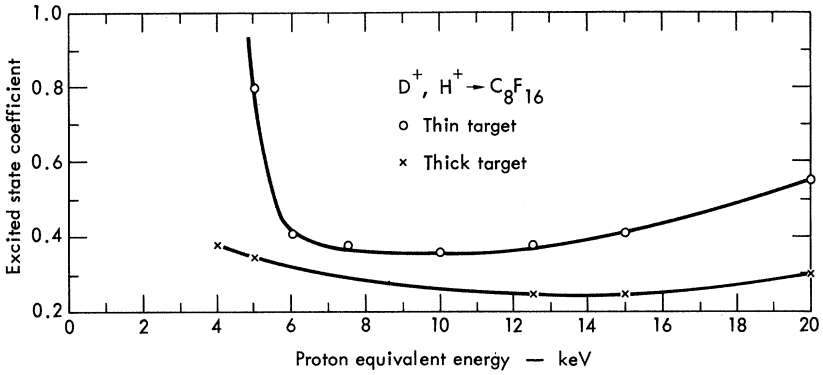

FIG. 14. Excited-state coefficient α as a function of proton equivalent energy for a target vapor of C_8F_{16}.

under somewhat different conditions, Riviere observed an increase in α at low energies for thick targets of C_8F_{16} and H_2.[11] Measurements of α as a function of target thickness were not given by Riviere for these gases.

A summary of our measured values of α for both thick and thin targets is given in Table I. Included in Table I are results of measurements on target vapors of C_8F_{16} and Freon 114. In Fig. 14, measurements of α for targets C_8F_{16} are presented in graphical form for both thin and thick targets. The thick-target results were measured with targets of the thickness indicated in Table I. For C_8F_{16}, α is observed to decrease as the target thickness is increased, contrary to the variation observed with gases H_2, N_2, NH_3, and H_2O. This observation suggests that loss of excited atoms by scattering dominates the enhancement of highly excited levels by multiple collisions when C_8F_{16} is the target gas.

CONCLUSION

We have measured excitation ratios and coefficients for atoms excited by charge exchange in thin targets and by multiple interactions in thick targets. These have been tabulated in Table I. Tentatively, it appears that excitation ratios may be enhanced at low energies by passage of the neutrals through a thick target – contrary to prior experience with more energetic particles. If this proves correct, selecting resonance or near-resonance charge-exchange conditions to produce maximum numbers of neutrals, which are then excited by interaction with thick-target atoms, may provide a better choice of neutralizer than at present, when excitation is designed to occur in the charge-exchange interaction. In addition, the thick-target neutral atoms provided to produce the excitation may be a different gas or vapor from that used for neutralization of the charged beam.

*Work performed under the auspices of the U. S. Atomic Energy Commission.

†Presently at University of Missouri, Rolla, Mo.

[1]D. R. Sweetman, Nucl. Fusion Suppl. 1, 279 (1962).

[2]A. H. Futch and C. C. Damm, Nucl. Fusion 3, 124 (1963).

[3]J. R. Hiskes, Phys. Rev. 137, A361 (1965).

[4]R. N. Il' in, V. A. Oparin, E. S. Solovev, and N. V. Fedorenko, Zh. Tekhn. Fiz. 36, 1241 (1966) [Soviet Phys. Tech. Phys. 11, 921 (1967)].

[5]K. H. Berkner, W. S. Cooper III, S. N. Kaplan, and R. V. Pyle, UCRL Report No. UCRL-18342, 1968 (unpublished).

[6]A. H. Futch and K. G. Moses, in *Fifth International Conference on the Physics of Electronic and Atomic Collisions* (Nauka, Leningrad, USSR, 1967), p. 12.

[7]A. C. Riviere, in Ref. 6, p. 15.

[8]J. R. Hiskes, in Ref. 6, p. 2.

[9]R. N. Il'in, B. I. Kikiani, V. A. Oparin, E. S. Solovev, and N. V. Fedorenko, Zh. Eksperim. i Teor. Fiz. 47, 1235 (1965) [Soviet Phys. -JETP 20, 835 (1965)].

[10]J. R. Hiskes, UCRL Report No. UCRL-7088 Rev. 1, 1964 (unpublished).

[11]A. C. Riviere (private communication).